

1 Urea-formaldehyde resin removal in medium density
2 fiberboards by steam explosion: developing non-
3 destructive analytical tools

4 *Sarah Troilo,^{†‡} Arnaud Besserer,[†] Christophe Rose[§], Safwan Saker[#], Lucas Soufflet,[‡] Nicolas
5 Brosse^{†*}*

6 [†]LERMAB, Université de Lorraine, INRAE, GP4W F54000 Nancy, France

7 [‡]CF2P, Zi Tertre Landry, 70200 Lure, France

8 [§]UMR 1137, Ecologie et Ecophysiologie Forestières, INRAe, 54280 Champenoux, France

9 [#]CRITT bois, 27 rue Philippe Seguin, F88000 Epinal, France

10

11 KEYWORDS

12 MDF waste, medium density fiberboards, UF resin removal, near-infrared spectroscopy,
13 correlative microscopy, fiber recovery

14

15 ABSTRACT

16 The cascading recycling of wood waste is currently a hot topic. Medium density fiberboard
17 (MDF) is a material whose consumption has been increasing worldwide for several decades.
18 However, current wood waste treatment processes do not allow for efficient recycling. The
19 potential of steam explosion (SE) treatment was investigated for stripping off the urea-
20 formaldehyde (UF) resin and the production of clean fibers from MDF. Hot liquid water during
21 the hydrothermal stage and water expansion during the decompression stage of SE provoked (1)
22 the hydrolytic breakdown of UF and the removal of > 80% of the resin from the fibers and (2)
23 efficient defibration of MDF producing $\approx 67\%$ of fibers with similar morphological features
24 when compared with MDF fibers. Near infrared spectroscopy (NIRS), nitrogen quantification
25 and confocal laser scanning microscopy/ scanning electron microscopy-wavelength dispersive
26 spectroscopy were used to evaluate the SE effect on UF removal from MDF fibers. The sample
27 clusters obtained by principal component analysis of NIRS spectra were correlated with nitrogen
28 content and processing conditions used. This work brings versatile solutions based on
29 hydrothermal treatments, namely SE, for diverse low environmental impact and valorization
30 routes of MDF waste. We showed that MDF processing treatment must be chosen wisely
31 according to the future valorization of the MDF targeted.

32

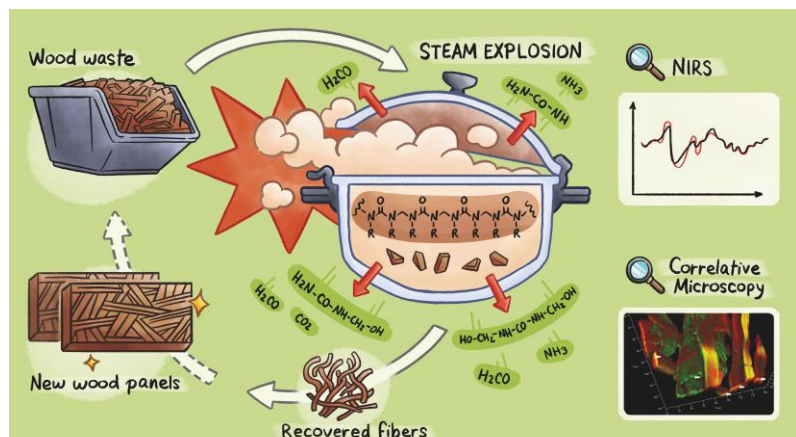
33

34

35

36

37 GRAPHICAL ABSTRACT



38
39
40

41 INTRODUCTION

42 Wood is a renewable material with valuable properties including recyclability. Current
43 consumption trends are leading to ever increasing volumes of waste wood, which may constitute
44 a feedstock for the cascade production of new products.¹ Among wood-based manufactured
45 products, medium density fiberboard (MDF) has been used since 1965 to produce a core stock
46 for the furniture industry.² Over the last few decades, household consumption habits have
47 changed as the lifespan of interior furniture has decreased. As a result, the world production of
48 fiberboard was multiplied by 4 between 2000 and 2020 and since 2015, the global production is
49 over 100 million m³.³ These evolutions have led to a sharp increase in waste furniture. For MDF
50 alone, the volume of waste generated in the last five years worldwide is estimated at 220 million
51 m³ and growing.⁴ However, unlike other wood products, there is no industrial scale process for
52 the recovery or recycling of MDF and most of the panels are currently incinerated or landfilled.
53 Recycling wood waste and especially MDF is challenging because of the presence of cured
54 residual adhesive on the surface of the fibers. The poor end-of-life management of MDF panels
55 has a negative environmental impact including the generation of hazardous gases during thermal
56 treatment and pollutants can be released into the environment.^{5,6} Recycling MDF is therefore a
57 major issue for the furniture industry and the wood sector in general.¹

58 Urea-formaldehyde (UF) resins are the most widely used in the wood sector because of their
59 high reactivity, good performance and low price.⁷ It has been shown in previous studies that the
60 presence of residual cured UF resin on the surface of the wood fibers negatively impacts the
61 properties of the panels formed from recycled wood.^{8,9} Cured UF resins have a relatively low
62 water resistance and can be degraded by hydrolysis.¹⁰ As a result, hydrolytic strategies have been

63 proposed for UF removal prior to the reuse of wood-based panels.¹¹ Neutral and acidic
64 hydrolysis can removed ~ 50% and ~ 70% respectively of UF resin from MDF fibers.¹²
65 Hydrothermal treatment led to a reduction in resin content but it also resulted in a reduction in
66 the average length and width of the fibers, thus reducing the potential for further fiber
67 recovery.^{13,14}

68 The steam explosion (SE) technology is both energy efficient and versatile. The technology was
69 initially developed to manufacture chipboard panels^{15,16} and is particularly mature for cellulosic
70 bioethanol^{1,17,18}. This process was also recently described for biomolecules and biopolymers
71 extraction or the valorization of biomass from phytotechnology.¹⁹⁻²² Several studies examined
72 the importance of water content in hydrolytic processes during SE pretreatments.^{23,24} However,
73 these phenomena are still largely unknown. The utilization of SE as a pretreatment for MDF
74 recovery was reported in the literature²⁵ but due to technical limitations, this study was carried
75 out at a relatively low pressure/temperature (0.16 MPa, 113°C). More recently, hydrolysis of UF
76 resin from wood waste during SE was studied.¹³ Temperature and steam ratio improved the UF
77 removal from waste, but neither the treatment homogeneity nor clear correlation could be
78 established between ammonia and formaldehyde emissions.

79 Processes for removing resin from wood must be coupled with effective technologies for
80 quantifying resin in the bulk and at the fiber scale. The cured resin is opaque and therefore
81 difficult to identify. Near-infrared spectroscopy (NIRS) is a promising non-destructive and
82 contactless method for waste wood sorting because it can distinguish treated wood from
83 untreated waste wood.^{26,27} Confocal laser scanning microscopy (CLSM) has been developed to
84 detect or visualize UF resin.²⁸ The combination of the localization of the region of interest by

85 CLSM and the morphology by scanning electron microscopy (SEM) is valuable to perform *in-*
86 *situ* analysis on the fibers. The elemental mapping analysis of nitrogen can be performed by
87 SEM coupled with energy dispersive spectroscopy (EDS) and its quantification achieved by
88 wavelength dispersive spectroscopy (WDS).²⁹

89 This work aims to examine and optimize the effect of SE processes performed at high pressure,
90 namely 0.9-1.9 MPa, on MDF waste. For an efficient recovery of MDF, two effects are sought:
91 the elimination of the glue on the surface of the fibers and the recovery of long (0.5 mm - 14
92 mm) wood fibers with a good yield. The impact of the treatment parameters on the fiber's
93 composition and the role of the water states in the hydrolytic degradation of the resin were
94 investigated. The study focused on a multi-processes approach that optimized resin removal,
95 maximized defibration and minimized the use of water to recover MDF fibers for future
96 recycling.

97 MATERIALS AND METHOD

98 **MDF characterization**

99 Because we wanted here to evaluate the UF removal potential of SE and decrease the variability
100 associated with the material, we used newly manufactured MDF. Standard MDF panels were
101 purchased from EGGER (EGGER Brilon GmbH & Co, Germany). The MDF samples were sawn
102 into cubes of side 20 mm to obtain sample sizes comparable to industrially ground waste wood
103 panels for recycling. The moisture content of the MDF samples was 6%.

104 **Resin removal and MDF fragmentation**

105 The experiments were carried out in two different reactors to optimize the resin removal and
106 MDF fragmentation.

107 The resin removal was optimized by a standard hydrothermal treatment. MDF samples were
108 treated by Hot Pressurized Water treatment (HPW) in a 10 L Parr reactor with a Parr 4842
109 temperature controller (Parr Instrument Company, Moline, IL, USA) at medium pressure (1
110 MPa) at 180°C for 15 minutes. Distilled water was in excess in the process to ensure the highest
111 resin removal rate. The ratio biomass/water was 1/25.

112 To optimize the fragmentation of the material and the water consumption, MDF samples were
113 treated by SE. Technically, the SE prototype used in this study (ADF, France) consists of a
114 steam generator that feeds the pressurized reactor containing the MDF to reach and maintain the
115 set temperature. The biomass was introduced horizontally in a 4.8 liters reactor and additional
116 water was injected into the pressurized SE reactor. Saturated steam at high pressure (1.6 MPa)
117 was injected in the reactor at 180°C for 15 minutes. The opening of a pneumatic valve dropped
118 the pressure in the reactor and the exploded biomass was released into the discharge tank (Figure
119 S1). The samples were treated by SE with additional water (SEW) with a ratio biomass/water
120 from 1/1 to 1/10.

121 To reduce the water consumption, SE experiments were carried out without the injection of
122 additional water with different retention times (from 5 to 20 minutes) and pressures (from 1.6 to
123 2.3 MPa). The results of the preliminary study were used to select the experimental conditions.

124 **Fibers drying**

125 As the SE generates effluents, the fibers had to be separated from the effluents and dried. The
126 fibers were separated from the liquid products by centrifugation at 7000 RPM for 10 min at room
127 temperature (Thermo Scientific Multifuge X4R Pro, USA). Supernatant was removed and kept
128 for subsequent analysis and fiber pellets were dried at 80°C for 24h and pressurized by air pulse.
129 Finally, fibers were sieved (300-850 μm mesh) and fiber size repartition was analyzed. The
130 complete process is depicted in Figure 1.



132 **Figure 1.** Process flowchart

133 **Pollutants quantification**

134 To determine the rate of UF-resin removal in different SE conditions, nitrogen and formaldehyde
135 were measured on the fibers. An elemental combustion analysis was performed on a Thermo
136 Scientific Flash EA 112 (USA) to determine the percentage of nitrogen on the fibers. The
137 samples were grounded into a homogeneous powder. The combustion of the samples was
138 performed at 950°C in the presence of copper oxide under oxygen flow for 15 seconds and
139 produces CO_2 , H_2O , SO_2 and NO_x which were reduced to nitrogen by copper. The combustion
140 products were then measured by gas chromatography under the conditions determined by the
141 manufacturer. The results were recorded and analyzed by the software Eager 300.

142 Formaldehyde emissions were measured according to the perforator method EN ISO 12460-5
143 (AFNOR, 2016) and a high-performance liquid chromatography (HPLC) method was used to
144 quantify the formaldehyde content on fibers after hydrothermal extraction. Previous works
145 showed UF resin can be efficiently extracted by hydrothermal treatment.^{14,30} Thus, the fibers

146 were autoclaved at 121°C for 20 min to extract the formaldehyde. Before the analysis, the
147 samples were derivatized with a solution of 2,4 dinitrophenylhydrazine (2,4 DNPH). 500 mg of
148 2,4 DNPH and 0.5 mL of phosphoric acid (H₃PO₄) 85% were dissolved in 49.5 mL of
149 acetonitrile. The pH of the samples was adjusted to 5. One milliliter of the sample was
150 centrifuged at 12 000 RPM for 10 min and the supernatant was passed through a 0.45 diameter
151 nylon filter. 20 µL of the sample, 30 µL of 2,4 DNPH solution and 950 µL of acetonitrile were
152 mixed in a 1.5 mL vial and injected into the HPLC. Formaldehyde analyses were performed on a
153 C18 Luna column (50 mm × 2.1 mm, 1.7 µm particle size) (Acquity, UPLC, Waters, USA) using
154 a HPLC (Thermo Scientific, Dionex Ultimate 3000, USA). The wavelength was set to 365 nm.
155 Separation was achieved with a mixture of water/acetonitrile (40:60, v/v). The flow rate was 0.3
156 mL/min and the injection volume was 1 µL. The total run time was 12 min.

157 **NIRS**

158 The measurements were performed on a Perkin Elmer NIRS spectrometer (USA) equipped with
159 an InGaAs detector and a CaF₂ beam splitter. Three samples of 5 g from each condition were
160 analyzed and five spectra for each sample were recorded from 10,000 to 4,000 cm⁻¹ with a 2 cm⁻¹
161 resolution. As described previously, only the spectral region between 6950 and 5500 cm⁻¹ was
162 further considered for analysis.³¹ The log₁₀ (1/R) of the spectral data was calculated. This
163 process is typically used for quantitative analysis.³² Then second derivative was calculated as
164 previously described.³³ In lab developed scripts based on RStudio and the plugin Chemospec
165 were used to analyze the raw data.³⁴ Principal component analysis (PCA) was performed to
166 analyze a limited set of independent and significant variables. The chemical differences of the
167 samples were visualized in a scatter plot and the loadings were analyzed to identify the main
168 contributive variables.

169 **CLEM**

170 In-situ analysis were performed by Correlative Light and Electron Spectroscopy (CLEM) to
171 observe the removal of the resin on the fibers by combining images from a CLSM and a SEM.
172 The sample were mounted on a stub accommodated on a specific holder (shuttle and find holder
173 for material sciences, Zeiss GmbH, Germany). The holder has three L-shaped registration
174 markers defining a coordinate system that can be quickly located and calibrated semi-
175 automatically in the "Shuttle & Find" module of Zen software (Zeiss GmbH, Germany) on both
176 CLSM and SEM microscopes. The areas of interest were first identified under a confocal
177 microscope and the images were saved including the "shuttle and find" coordinate system. Then
178 the same areas of interest were recovered under the SEM (Sigma HDVP and EVO 15, Zeiss
179 GmbH, Germany) to perform electronic imaging and microanalysis with an EDS (SDD X max
180 80mm², Oxford instrument, UK) and a WDS detector (IncaWave 600, Oxford instrument, UK).
181 To perform spectral deconvolution, samples were stained in 0.1% aqueous safranin O (Merck)
182 for 5 min and rinsed until the water became clear. They were mounted onto SEM specimen stubs
183 and observed on a confocal LSM 780 r (Zeiss GmbH, Germany) equipped with a spectral
184 deconvolution mode. The settings were optimized to ensure maximum distinction between
185 stained resin and fibers into green and red emission light, respectively. Uncoated-control fibers,
186 UF coated-control fibers and UF-resin were used as references and were compared to SE treated
187 samples.

188 After the observation on the confocal microscope and prior to the observations on the SEM, the
189 samples were coated under a high vacuum mode with 2 nm of platinum (ACE600 metallizer,
190 LEICA, Germany).

191 **EDS and WDS analyses**

192 The field of observation was relocated to a FE-SEM (Sigma HDVP, Zeiss GmbH, Germany) to
193 perform EDS analysis and then under an EVO15-SEM equipped with a WDS detector (Zeiss
194 GmbH, Germany). The WDS is an INCA Wave that can accommodate six crystals and is
195 equipped with a crystal optimized for nitrogen analysis LSM80E (Oxford Instruments, UK).
196 Surface images for the selection of sites of interest were acquired from a high definition back-
197 scattered detector (HDBSD) (Zeiss GmbH, Germany).

198 The working distance on the EVO15 was 9 mm. The acceleration voltage and the beam current
199 were set to 10 Kv and 5 nA respectively for the nitrogen measurements performed on the fibers.
200 The specific peaks of nitrogen were acquired and deconvoluted with the Energy+ 250 interface
201 of the INCA software. The calibration and the optimization of the detection of the nitrogen peak
202 were carried out under the conditions of acquisition starting from a pellet of glue powder with
203 the WAVE interface of the INCA software suite (Oxford Instruments). For each sample, the
204 relative elemental percentage of nitrogen was measured on 9 pellets of 8 mm diameter and 0.5
205 mm thickness. The reference used for nitrogen content was cured UF resin.

206 **X-ray tomography**

207 One cube of side 20 mm was scanned on a 39 Watt Tomograph (RX Solution, France) with a
208 high tension of 0–130 kW and an anode current of 0–300 μ A. The voxel size was 10.67 μ m. A
209 subsample of 500 slices amongst the 1131 slices was selected for the 3D reconstruction using
210 Fiji software³⁵.

211

212 RESULTS AND DISCUSSION

213 **Hot Pressurized Water treatment (HPW)**

214 In a first attempt, the effect of a standard hydrothermal treatment (i.e without decompressive
215 explosion) was experimented by treating MDF samples by HPW in a closed high-pressure
216 reactor at 180°C for 15 min (Table 1, run 1). Perforator extraction coupled with HPLC analysis
217 showed a total removal of formaldehyde emissions after treatment (2.4 mg/100 g of dry mass
218 MDF before treatment to non-detectable after HPW). Hydrolysis of UF resin was reported to
219 produce mainly urea, ammonia and formaldehyde.¹³ Quantification of nitrogen by the Kjeldahl
220 method was used as an indicator of resin removal performance. HPW led to a 91% (\pm 1%)
221 reduction in nitrogen content (Table 1) and to a 94 % reduction in formaldehyde content (\pm 1%)
222 in the fiber.

223 In order to analyze the effect of the treatment on the fragmentation of the sample, a defibration
224 class (dc) was defined as followed: 0 = unaltered sample, 1 = sample swelling, 2 = partial
225 defibration and 3 = total defibration. As shown in Table 1 and Figure 2, HPW treatment of MDF
226 led to a swelling of the sample without disruption of MDF ultra-structure (defibration class = 1,
227 Table 1). However, the fragmentation of the material can be required for the future use of the
228 recovered fibers.



230 **Figure 2.** Effect of the treatment on the MDF fragmentation and defibration class definition, 0 =
 231 unaltered sample, 1 = sample swelling, 2 = partial defibration, 3 = total defibration.

232

233 **Steam explosion treatment (SE and SEW)**

234 MDF was treated by SE using 4 temperatures and 4 residence times as summarized in Table 1
 235 (runs 2-10). The condition sets used in this study were selected considering a visual effect of the
 236 material. Technically, the SE pilot consists of a steam generator that feeds the pressurized reactor
 237 containing the MDF to reach and maintain the set temperature. During the explosive discharge,
 238 the fibers are recovered in the explosion tank with condensed water. For the runs 11-15 (SEW),
 239 the water content was increased by injection of additional water in the pressurized SE reactor
 240 before heating by steam injection.

241 **Table 1.** HPW, SE and SEW with reaction conditions and nitrogen content.

Run	Process	Pressure (MPa)	T (°C)	t (min)	S/L	N (% of total elements)	N removal (%)	Defibration class
MDF						4.15 ± 0.03		0
1	HPW	1.6	180	15	1/25	0.40 ± 0.03	-92%	1
2	SE	1.6	180	10		1.00 ± 0.01	-76%	2
3	SE	1.6	180	15		1.27 ± 0.01	-69%	3
4	SE	1.6	180	20		0.70 ± 0.02	-83%	3
5	SE	1.9	190	5		0.83 ± 0.01	-80%	3

6	SE	1.9	190	10		0.91 ± 0.01	-78%	3
7	SE	1.9	190	20		1.02 ± 0.05	-75%	3
8	SE	2.3	200	5		1.65 ± 0.01	-65%	3
9	SE	2.3	200	10		1.09 ± 0.03	-74%	3
10	SE	2.8	210	5		1.88 ± 0.04	-55%	3
<hr/>								
11	SEW	1.6	180	15	1/1	0.78 ± 0.04	-81%	3
12	SEW	1.6	180	15	1/2	0.80 ± 0.03	-81%	3
13	SEW	1.6	180	15	1/6	0.60 ± 0.02	-86%	3
14	SEW	1.6	180	15	1/8	0.64 ± 0.01	-85%	3
15	SEW	1.6	180	15	1/10	0.59 ± 0.01	-86%	3

242

243 Standardized analysis (see Materials and Method section) showed that formaldehyde emissions

244 from all SE and SEW treated fibers were below the detection limit. Regarding the evaluation of

245 the efficiency of the resin removal, nitrogen quantifications were carried out. As seen in Table 1,

246 SE treatment (runs 2-10) allowed the removal of 55 %-83 % of the resin from the fibers. For run

247 2, performed at the lowest SE severity a partial defibration of MDF was observed (see Fig. 2). In

248 contrast, runs 3-10 allowed total defibration (Fig. 2.) probably because of the explosive

249 decompression step, involving a well-known water expansion. As previously proposed in a study

250 aiming at the defibration of bast fibers, the high-speed extrusion of MDF from the reactor to the

251 cyclone during the explosive decompression could also induce a high mechanical stress to the
252 material causing its total disruption³⁶.

253 Interestingly, it was observed that a decrease of the ratio solid: liquid improved the removal of
254 the resin. A comparison of run 3 and runs 11-15 showed that a SEW carried out with the same
255 severity but with a higher water content resulted in a significant decrease in N%, from $\approx 1.3\%$ to
256 $\approx 0.6-0.8\%$ which correspond to the removal of $\approx 85\%$ of the resin. This observation is in line
257 with previous works dealing with the SE pre-treatment of lignocellulosic biomass. These studies
258 have shown that an increase in condensed water content during the cooking step of SE could
259 promote hydrolysis reactions through autohydrolysis mechanisms.²³ However, Table 1 shows
260 that resin removal reached a limit and that from a 1: 6 ratio onwards, increasing the volume of
261 water did not significantly improve adhesive removal (runs 14 and 15). Increasing the severity
262 of steam treatments allowed a gradual removal of resin up to 80% and that a further increase of
263 severity did not improve the resin removal.¹⁴ In accordance with this work, it appeared from our
264 study that $\approx 15-20\%$ of the UF is strongly linked to the fibers and is highly recalcitrant.

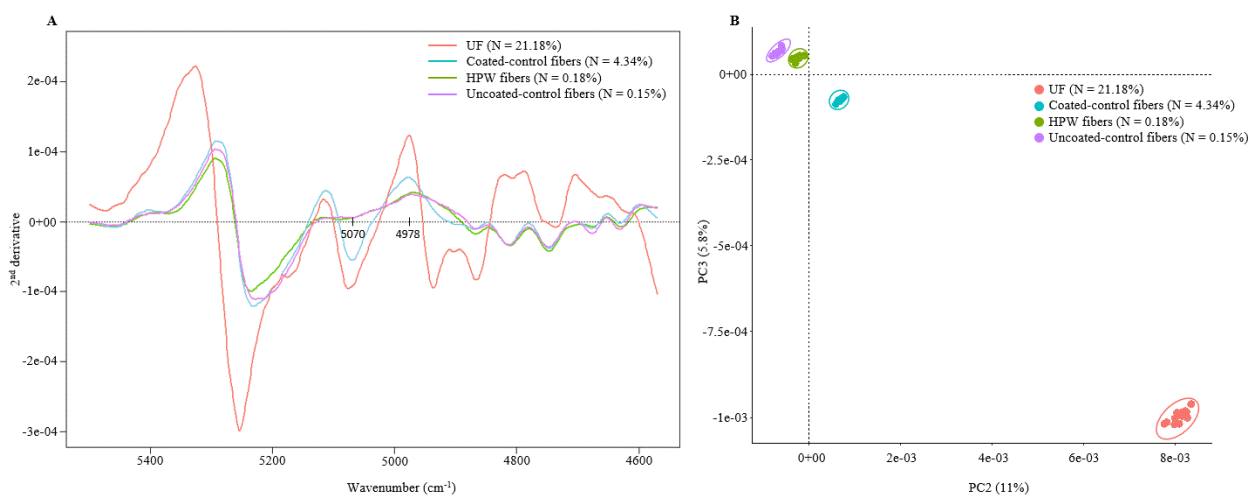
265 **NIRS characterization**

266 NIRS which was successfully used to describe UF synthesis was experimented in this work as a
267 non-destructive technique to characterize samples subjected to HPW and SE treatments.³⁷ NIRS
268 acquisition (n = 15) were first performed on uncoated-control fibers, coated-control fibers
269 (containing UF resin) and treated by HPW (positive control of the resin removal) and compared
270 with cured UF resin. A PCA was performed on the second derivative spectra. Based on the signal
271 to noise ratio of the spectra, spectral region of interest was selected between 7000 cm^{-1} and 4500
272 cm^{-1} (Figure S2). The variability analysis showed three spectral regions with high variability: one

273 between 6858 cm^{-1} and 6630 cm^{-1} , another one between 5978 cm^{-1} and 5726 cm^{-1} and the last
274 one between 5500 cm^{-1} and 4570 cm^{-1} (Figure S3).

275 In order to determine the best conditions for analysis, PCA was performed on each subregion.
276 Plotting of PCA of the components 1 and 2 performed on the region between 5500 cm^{-1} and
277 4570 cm^{-1} allowed the best discrimination between wood and resin materials (Figure S4) but the
278 best correlation between NIRS samples clusters and nitrogen content was obtained for the area
279 between 5500 cm^{-1} and 4570 cm^{-1} (Fig. 3A) with components 2 and 3 plotted. This subregion has
280 thus been selected for subsequent analysis. As shown on figure 3B, after PCA samples fall in
281 significant distinct clusters that were correlated with their relative nitrogen content.

282



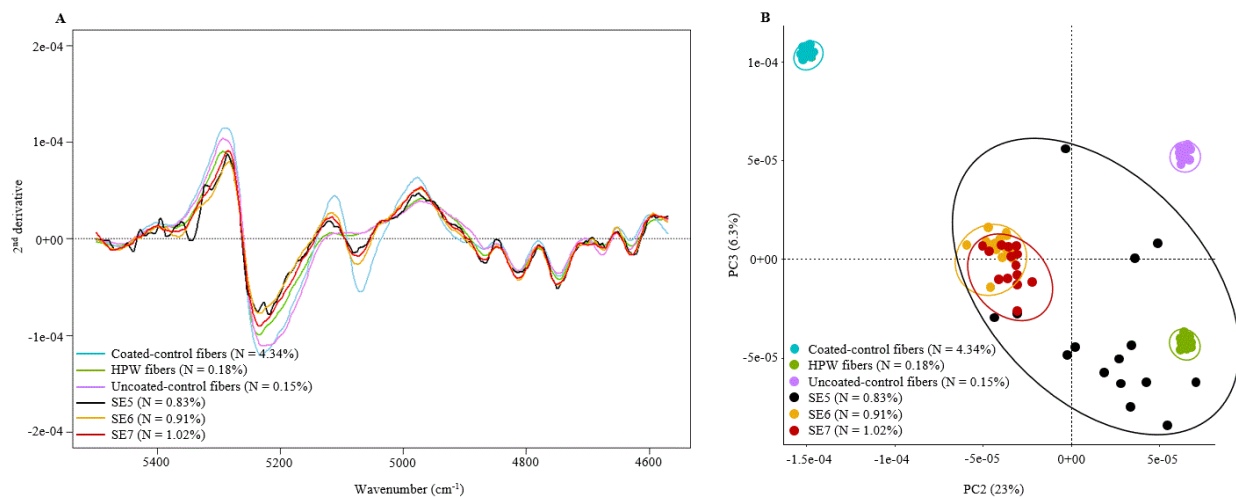
283

284 **Figure 3.** NIRS detection of UF resin in MDF samples. A) Mean second derivative of cured UF
285 (red), coated-control fibers (blue), HPW (green) and uncoated-control fibers (violet). The mean
286 second derivative was calculated between 5500 cm^{-1} and 4570 cm^{-1} ; n=15. B) PCA of cured UF,
287 coated-control fibers, HPW and uncoated-control fibers. The plot shows PC2-PC3 scores.

288 Variability analysis of the mean second derivative spectra and loadings analysis showed that the
289 bands at 5070 cm^{-1} and 4978 cm^{-1} were found to be present in cured UF and in coated-control
290 fibers but not in uncoated-control fibers (Fig. 3A and S5). These bands were found to be
291 significant contributors to the variance explained on principal components 2 and 3 (Figure S5).
292 These bands have thus been used as a marker of UF resin in subsequent analysis.

293 NIRS analysis was then performed on fibers treated by SE. Combining variability analysis and
294 loadings analysis from PCA allowed to validate the attribution of the bands 5070 cm^{-1} and 4978
295 cm^{-1} to the resin (Figure S6). The plotting of the spectral region (Fig. 4A) showed clearly a
296 decrease of the amplitude of UF resin marker bands in all samples proceed by SE.

297 Plotting of PCA of the components 2 and 3 (Fig. 4B) confirmed trends observed on second
298 derivative spectra (Fig. 4A). NIRS allowed discrimination of samples in clusters according to the
299 treatment parameters. HPW fibers were really closed to uncoated-control fibers and SE fibers fall
300 in an intermediate cluster between coated-control fibers and HPW. The fibers treated by SE at
301 190°C for 10 and 20 min are not discriminated. The high dispersion of the fibers treated by SE at
302 190°C for 5 min reflected the high variability of the treatment. Interestingly, the variability of the
303 sample (95% CI ellipses) was decreasing with the increase of the residence time in the reactor.
304 The tighter the scatter plot, the more homogeneous the treatment. Thus, increasing the retention
305 time from 5 to 10 minutes allowed to improve the homogeneity of the treatment without
306 decreasing thermohydrolysis efficiency of UF resin. Taking together, treating the fibers at 190°C
307 for 10 min allowed to obtain a good compromise between the retention time, the homogeneity of
308 the treatment, the resin removal and the defibration of the material.



309
 310 **Figure 4.** NIRS monitoring of SE effect on MDF fibers. A) Second derivative, B) PCA of
 311 coated-control fibers, HPW, uncoated-control fibers, SE5, SE6 and SE7 fibers. The mean second
 312 derivative was calculated between 5500 cm⁻¹ and 4500 cm⁻¹ (n=15). The plot shows PC2 and
 313 PC3 scores. For each cluster the nitrogen content is indicated.

314 **Fibers yield, morphology and resin mapping**

315 Hydrothermal treatments previously described in the literature on MDF recycling lead to a fiber
 316 shortening of ~ 30%¹¹. Steam refining performed in comparable conditions lead to a fiber yield
 317 of ~ 75%¹⁴. In this study, regardless of the experimental SE or SEW conditions considered
 318 (Table 1, runs 2-15), a comparable fiber yield of 80% w/w (± 2 %) was achieved. Regarding the
 319 fibers morphology, fibers resulting from run 6 were further analyzed. The fiber size distribution
 320 is reported in Table 2. The size of the wood fibers used in the manufacture of MDF panels is
 321 between 0.5 and 6 mm depending on the wood species and the manufacturing process used³⁸. A
 322 picture of the three fiber fractions obtained after SE 6 is given in Figure S7. For comparison, X-
 323 ray tomography of the wood fibers in the MDF panel board was done (Fig S7A). Interestingly, in
 324 these conditions SE allowed the recovery of more than 67% of the fibers with a length above 300

325 μm without visible alteration of the fiber morphology. The different fiber fractions could be
326 reused in different applications such as new panels or bio based composite materials.

327 **Table 2.** Particle size distribution of MDF fibers treated by SE (run SE6)

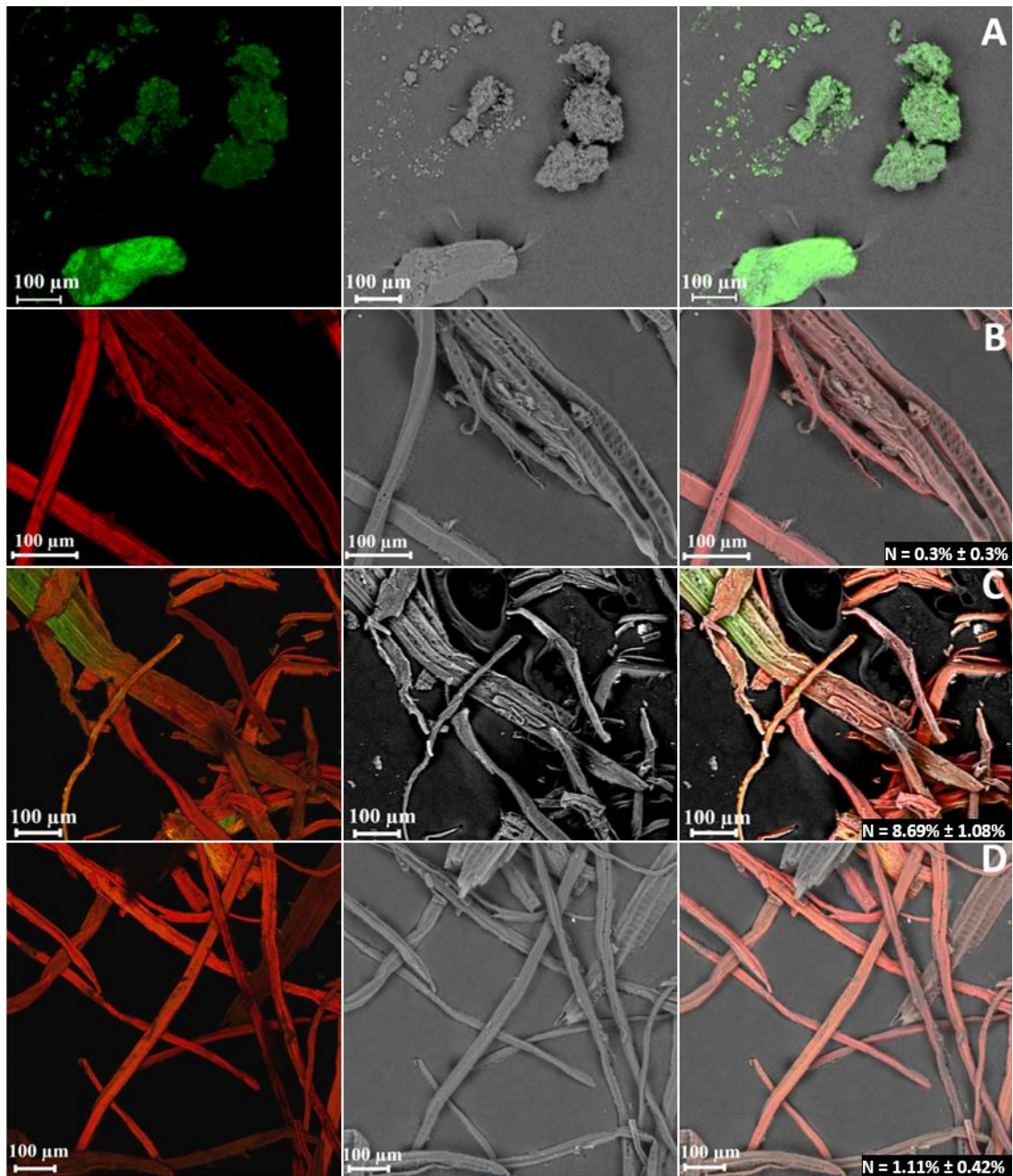
Sieve Mesh	Fraction type	Material captured
> 850 μm	Coarse fibers (a)	28% \pm 3%
300 μm – 800 μm	Medium coarse fibers (b)	35% \pm 3%
< 300 μm	Fines (c)	37% \pm 7%

328

329 To map the UF resin on the fibers, optical fluorescence microscopy was used. A preliminary
330 study was carried out to validate the staining method using safranin. Safranin-stained unresinated
331 fibers and UF resin were observed under a confocal microscope to acquire specific fluorescence
332 emission spectra. The maxima emission of the resin and the wood being distinct, it is possible to
333 apply a spectral deconvolution at any pixel of the microscope image in order to attribute a signal
334 to the resin (green) (Fig. 5A) and to the wood (red) (Fig. 5B). Indeed, after staining, the cell
335 walls of wood containing cellulose and lignin produced a red fluorescence.³⁹ The fiber staining
336 method made it possible to visualize the distribution of resin on MDF fibers with high sensitivity
337 and specificity.⁴⁰ It is therefore suitable for comparing non-treated MDF fibers with a high
338 amount of UF resin and treated MDF fibers (run SE6) with a residual amount of UF resin.

339 The images on Figure 5 are representative of the observed phenomenon. coated-control fibers
340 (Fig. 5C) showed green patches on wood fiber in red. This patchy distribution of UF resin was
341 observed previously.^{41,42} In order to validate that green signal was resulting from UF resin
342 occurrence, correlative CLSM-SEM microscopy coupled to WDS analysis was carried out.

343 Briefly, after observation of fields of interest with CLSM, these fields could be relocated under
344 the SEM and an overlay of the two images could be obtained. Then EDS and WDS spectral
345 acquisition could be done on specific region of interest on fibers or fiber pellets. CLEM-EDS and
346 WDS microanalysis confirmed the localization of nitrogen coming from UF in the green areas
347 (Figure S8, S9). These observations validate the methodology. Treated fibers (SE6, Fig. 5D)
348 displayed a strong decrease of the green fluorescence linked to the resin and instead showed a
349 yellow orange fluorescence. Three dimensional reconstructions showed the intrinsic embedding
350 of the UF resin in the fiber making its total removal impossible without destroying the fibers
351 (Figure S10) and are in agreement with the previous reports of UF resin penetration into the
352 fibers leading to its recalcitrance^{14,43}. These images confirmed an efficient resin removal from
353 the steam exploded fibers.



354

355 **Figure 5.** From left to right, CLSM (maximal intensity projection), SEM and CLEM images of

356 A) UF resin B) Uncoated-control fibers C) Coated-control fibers and D) Treated MDF fibers

357 SE6, stained by safranin. Relative nitrogen percentage determined by WDS on fibers pellets,

358 mean of 15 acquisitions are given on CLEM images. Error values are 95% CI.

359 CLEM-EDS allowed the UF mapping on fibers but is not quantitative. Thus, SEM-WDS
360 quantification was performed on pellets of milled fibers. Relative nitrogen quantifications are
361 indicated in Figure 5. Interestingly, fibers resulting from SE6 treatment differed significantly
362 from coated-control fibers but not from uncoated-control fibers (ANOVA, $P = 0.81$). This non-
363 destructive *in-situ* semi-quantitative analysis estimated a relative resin removal on the fibers
364 treated by SE of about 88% which is in the same range as the bulk elemental combustion
365 analysis.

366 CONCLUSION

367 Compared to hot pressurized water treatment, steam explosion is a very promising process for
368 the recovery of MDF fibers, allowing 83% of the resin removal accompanied with an efficient
369 fragmentation in a very short time and a water consumption divided by 3. MDF waste must be
370 treated according to its future recovery to choose the most suitable treatment. A detailed analysis
371 of the fibers was conducted to characterize the fibers. PCA performed on NIRS data has great
372 potential for distinguishing waste MDF and recovered fibers. The loadings analysis confirmed
373 the decrease of the resin on recovered fibers. Combining CLSM and SEM allowed the
374 observation and *in situ* quantification of the reduction of UF resin coverage on MDF fibers. The
375 work that we are currently carrying out in the perspective of industrial developments aim to (1)
376 validate the results obtained on real MDF waste; (2) take interest in the decontamination of the
377 aqueous effluents of the process which were not addressed in this article; (3) transfer the batch
378 process into a continuous process. We hope that these prospects will pave the way for industrial
379 recycling of MDF with a better environmental impact than its current end-of-life management.

380 ASSOCIATED CONTENT

381 **Supporting information.** The supporting information is available free of charge on the ACS
382 Publication website.

383 Steam explosion schematic view. Determination of the informative region of second derivative
384 spectra. Variability analysis on second derivative spectra calculated between 7000 cm⁻¹ and
385 4500 cm⁻¹ and identification of the three sub regions of interest. PCA analysis with PC1 and
386 PC2. Variability and loadings analysis for UF bands identification between 5500 cm⁻¹ and 4570
387 cm⁻¹. Variability and loadings analysis on SE and HPW samples between 5500 cm⁻¹ and 4570
388 cm⁻¹. Fibers treated by SE6. CLEM-EDS analysis of UF-resin on wood fibers. CLEM-EDS
389 analysis of UF-resin on wood fibers with EDS nitrogen mapping. CLSM 3D reconstruction of
390 MDF fibers.

391

392 AUTHOR INFORMATION

393 **Corresponding Author**

394 Nicolas Brosse

395 E-mail: nicolas.brosse@univ-lorraine.fr

396

397

398 **Author Contributions**

399 Sarah Troilo: Investigation and Conceptualization. Arnaud Besserer: Methodology. Analysis.

400 Investigation. Christophe Rose: Investigation and analysis. Safwan Saker: technical assistance.

401 Lucas Soufflet: Project administration and funding. Nicolas Brosse: Project administration and
402 supervision.

403 **Notes**

404 The authors declare no competing financial interest.

405 **Funding Sources**

406 EA 4370 LERMAB is supported by the French National Research Agency through the ARBRE
407 Laboratory of Excellence (ANR-12-LABXARBRE-01). The authors thank the “Association
408 Nationale Recherche Technologie” (ANRT) and the French company CF2P for funding provided
409 to this research program.

410 ACKNOWLEDGMENT

411 The authors would like to thank SILVATECH (Silvatech, INRAE, 2018. Structural and
412 functional analysis of tree and wood Facility, doi: 10.15454/1.5572400113627854E12) from
413 UMR 1434 SILVA, 1136 IAM, 1138 BEF and 4370 EA LERMAB from the research center
414 INRAE Grand-Est Nancy for its contribution to microscope observation and microanalysis.
415 SILVATECH facility is supported by the French National Research Agency through the
416 Laboratory of Excellence ARBRE (ANR-11-LABX-0002-01).

417 ABBREVIATIONS

418 CLEM, correlative light electron microscopy; CLSM, confocal laser scanning microscopy; EDS,
419 energy dispersive spectroscopy; HPLC, high-performance liquid chromatography; HPW, hot
420 pressurized water treatment; MDF, medium density fiberboard; NIRS, near-infrared
421 spectroscopy PCA, principal component analysis; SE, steam explosion; SEM, scanning electron
422 microscopy, SEW, steam explosion with additional water; UF, urea-formaldehyde; WDS,
423 wavelength-dispersive spectroscopy.

424 REFERENCES

- 425 (1) Besserer, A.; Troilo, S.; Girods, P.; Rogaume, Y.; Brosse, N. Cascading Recycling of Wood
426 Waste: A Review. *Polymers* **2021**, *13* (11), 1752. <https://doi.org/10.3390/polym13111752>.
- 427 (2) Suchsland, O. *Fiberboard Manufacturing Practices in the United States*; U.S. Department
428 of Agriculture, Forest Service, 1987; Vol. 640.
- 429 (3) FAOSTAT. *Forestry Production and Trade*. <http://www.fao.org/faostat/en/#data/FO>
430 (accessed 2021-10-05).

- 431 (4) Irle, M.; Privat, F.; Couret, L.; Belloncle, C.; D eroubaix, G.; Bonnin, E.; Cathala, B.
432 Advanced Recycling of Post-Consumer Solid Wood and MDF. *Wood Material Science &*
433 *Engineering* **2019**, *14* (1), 19–23. <https://doi.org/10.1080/17480272.2018.1427144>.
- 434 (5) Girods, P.; Rogaume, Y.; Dufour, A.; Rogaume, C.; Zoulalian, A. Low-Temperature
435 Pyrolysis of Wood Waste Containing Urea–Formaldehyde Resin. *Renewable Energy* **2008**,
436 *33* (4), 648–654. <https://doi.org/10.1016/j.renene.2007.03.026>.
- 437 (6) Lee, M.; Prewitt, L.; Mun, S. P. Formaldehyde Release from Medium Density Fiberboard
438 in Simulated Landfills for Recycling. *Journal of the Korean Wood Science and Technology*
439 **2014**, *42* (5), 597–604. <https://doi.org/10.5658/WOOD.2014.42.5.597>.
- 440 (7) Dunky, M. Urea–Formaldehyde (UF) Adhesive Resins for Wood. *International Journal of*
441 *Adhesion and Adhesives* **1998**, *18* (2), 95–107. [https://doi.org/10.1016/S0143-
442 *7496\(97\)00054-7*.](https://doi.org/10.1016/S0143-7496(97)00054-7)
- 443 (8) Moezzi-pour, B.; Ahmadi, M.; Abdolkhani, A.; Doosthoseini, K. Chemical Changes of
444 Wood Fibers after Hydrothermal Recycling of MDF Wastes. *J Indian Acad Wood Sci* **2017**,
445 *14* (2), 133–138. <https://doi.org/10.1007/s13196-017-0198-6>.
- 446 (9) Zhong, R.; Gu, J.; Gao, Z.; Tu, D.; Hu, C. Impacts of Urea-Formaldehyde Resin Residue on
447 Recycling and Reconstitution of Wood-Based Panels. *International Journal of Adhesion*
448 *and Adhesives* **2017**, *78*, 60–66. <https://doi.org/10.1016/j.ijadhadh.2017.06.019>.
- 449 (10) Fleischer, O.; Marutzky, R. Hydrolyse von Harnstoff-Formaldehyd-Harzen: Auflo sung
450 des Spangefu ges in Holzwerkstoffen durch hydrolytischen Abbau der Leimfuge. *Holz Als*
451 *Roh Und Werkstoff* **2000**, *6*.
- 452 (11) Lubis, M. A. R.; Manohar, S. Y.; Laksana, R. P. B.; Fatriasari, W.; Ismayati, M.; Falah, F.;
453 Solihat, N. N.; Sari, F. P.; Hidayat, W. The Removal of Cured Urea-Formaldehyde
454 Adhesive towards Sustainable Medium Density Fiberboard Production: A Review. *JSL*
455 **2021**, *9* (1), 23. <https://doi.org/10.23960/jsl1923-44>.
- 456 (12) Lubis, M. A. R.; Hong, M.-K.; Park, B.-D. Hydrolytic Removal of Cured Urea–
457 Formaldehyde Resins in Medium-Density Fiberboard for Recycling. *Journal of Wood*
458 *Chemistry and Technology* **2018**, *38* (1), 1–14.
459 <https://doi.org/10.1080/02773813.2017.1316741>.
- 460 (13) Gibier, M.; Sadeghisadeghabad, M.; Girods, P.; Zoulalian, A.; Rogaume, Y. Furniture
461 Wood Waste Depollution through Hydrolysis under Pressurized Water Steam:
462 Experimental Work and Kinetic Modelization. *Journal of Hazardous Materials* **2022**, *436*,
463 129126. <https://doi.org/10.1016/j.jhazmat.2022.129126>.
- 464 (14) Hagel, S.; Saake, B. Fractionation of Waste MDF by Steam Refining. *Molecules* **2020**, *25*
465 (9), 2165. <https://doi.org/10.3390/molecules25092165>.
- 466 (15) Mason, W. H. Process and Apparatus for Disintegration of Wood and the Like, 1926.
467 <https://patentimages.storage.googleapis.com/0a/31/f4/551e24519451f0/US1578609.pdf>
468 (accessed 2020-07-20).
- 469 (16) Ziegler-Devin, I.; Chrusciel, L.; Brosse, N. Steam Explosion Pretreatment of
470 Lignocellulosic Biomass: A Mini-Review of Theoretical and Experimental Approaches.
471 *Frontiers in Chemistry* **2021**, *9*, 860. <https://doi.org/10.3389/fchem.2021.705358>.
- 472 (17) Fernandes, M. C.; Ferro, M. D.; Paulino, A. F. C.; Mendes, J. A. S.; Gravitis, J.; Evtuguin,
473 D. V.; Xavier, A. M. R. B. Enzymatic Saccharification and Bioethanol Production from
474 *Cynara Cardunculus* Pretreated by Steam Explosion. *Bioresource Technology* **2015**, *186*,
475 309–315. <https://doi.org/10.1016/j.biortech.2015.03.037>.

- 476 (18) Chen, W.-H.; Pen, B.-L.; Yu, C.-T.; Hwang, W.-S. Pretreatment Efficiency and Structural
477 Characterization of Rice Straw by an Integrated Process of Dilute-Acid and Steam
478 Explosion for Bioethanol Production. *Bioresource Technology* **2011**, *102* (3), 2916–2924.
479 <https://doi.org/10.1016/j.biortech.2010.11.052>.
- 480 (19) Chadni, M.; Grimi, N.; Bals, O.; Ziegler-Devin, I.; Brosse, N. Steam Explosion Process for
481 the Selective Extraction of Hemicelluloses Polymers from Spruce Sawdust. *Industrial*
482 *Crops and Products* **2019**, *141*, 111757. <https://doi.org/10.1016/j.indcrop.2019.111757>.
- 483 (20) He, Q.; Ziegler-Devin, I.; Chrusciel, L.; Obame, S. N.; Hong, L.; Lu, X.; Brosse, N. Lignin-
484 First Integrated Steam Explosion Process for Green Wood Adhesive Application. *ACS*
485 *Sustainable Chem. Eng.* **2020**, *8* (13), 5380–5392.
486 <https://doi.org/10.1021/acssuschemeng.0c01065>.
- 487 (21) Mouguala Moukagni, E.; Ziegler-Devin, I.; Safou-Tchima, R.; Brosse, N. Extraction of
488 Acetylated Glucuronoxylans and Glucomannans from Okoume (*Aucoumea Klaineana*
489 Pierre) Sapwood and Heartwood by Steam Explosion. *Industrial Crops and Products* **2021**,
490 *166*, 113466. <https://doi.org/10.1016/j.indcrop.2021.113466>.
- 491 (22) Simangunsong, E.; Ziegler-Devin, I.; Chrusciel, L.; Girods, P.; Wistara, N.; Brosse, N.
492 Steam Explosion of Beech Wood: Effect of the Particle Size on the Xylans Recovery |
493 EndNote Click. **2020**.
- 494 (23) Sui, W.; Chen, H. Effects of Water States on Steam Explosion of Lignocellulosic Biomass.
495 **2016**.
- 496 (24) Liu, L.-Y.; Qin, J.-C.; Li, K.; Mehmood, M. A.; Liu, C.-G. Impact of Moisture Content on
497 Instant Catapult Steam Explosion Pretreatment of Sweet Potato Vine. **2017**.
498 <https://doi.org/10.14288/1.0360749>.
- 499 (25) Wan, H.; Wang, X.-M.; Barry, A.; Shen, J. Recycling Wood Composite Panels:
500 Characterizing Recycled Materials. *BioResources* **2014**, *9*.
501 <https://doi.org/10.15376/biores.9.4.7554-7565>.
- 502 (26) Mauruschat, D.; Plinke, B.; Aderhold, J.; Gunschera, J.; Meinschmidt, P.; Salthammer, T.
503 Application of Near-Infrared Spectroscopy for the Fast Detection and Sorting of Wood–
504 Plastic Composites and Waste Wood Treated with Wood Preservatives. *Wood Sci Technol*
505 **2016**, *50* (2), 313–331. <https://doi.org/10.1007/s00226-015-0785-x>.
- 506 (27) So, C.-L.; Lebow, S. T.; Groom, L. H.; Rials, T. G. The Application of near Infrared (NIR)
507 Spectroscopy to Inorganic Preservative-Treated Wood. *Wood and Fiber Science* **2004**,
508 *36*(3), 329–336.
- 509 (28) Pakdel, H.; Cyr, P.-L.; Riedl, B.; Deng, J. Quantification of Urea Formaldehyde Resin in
510 Wood Fibers Using X-Ray Photoelectron Spectroscopy and Confocal Laser Scanning
511 Microscopy. *Wood Sci Technol* **2008**, *42* (2), 133–148. <https://doi.org/10.1007/s00226-007-0155-4>.
- 513 (29) Tessier, F. Determining the Nitrogen Content in (Oxy)Nitride Materials. *Materials* **2018**, *11*
514 (8), 1331. <https://doi.org/10.3390/ma11081331>.
- 515 (30) Ren, T.; Wang, Y.; Wu, N.; Qing, Y.; Li, X.; Wu, Y.; Liu, M. Degradation of Urea-
516 Formaldehyde Resin Residues by a Hydrothermal Oxidation Method into Recyclable Small
517 Molecular Organics. *Journal of Hazardous Materials* **2022**, *426*, 127783.
518 <https://doi.org/10.1016/j.jhazmat.2021.127783>.
- 519 (31) Fackler, K.; Schwanninger, M.; Gradinger, C.; Srebotnik, E.; Hinterstoisser, B.; Messner,
520 K. Fungal Decay of Spruce and Beech Wood Assessed by Near-Infrared Spectroscopy in

- 521 Combination with Uni- and Multivariate Data Analysis. *Holzforschung* **2007**, *61* (6), 680–
522 687. <https://doi.org/10.1515/HF.2007.098>.
- 523 (32) Schwanninger, M.; Rodrigues, J. C.; Fackler, K. A Review of Band Assignments in near
524 Infrared Spectra of Wood and Wood Components. *Journal of Near Infrared Spectroscopy*
525 **2011**, *19* (5), 287–308. <https://doi.org/10.1255/jnirs.955>.
- 526 (33) Sandak, A.; Sandak, J.; Zborowska, M.; Prądyński, W. Near Infrared Spectroscopy as a
527 Tool for Archaeological Wood Characterization. *Journal of Archaeological Science* **2010**,
528 *37* (9), 2093–2101. <https://doi.org/10.1016/j.jas.2010.02.005>.
- 529 (34) Hanson, B. A. ChemoSpec: An R Package for Chemometric Analysis of Spectroscopic
530 Data (Package Version 4.4.97), 2017. <https://bryanhanson.github.io/ChemoSpec/> (accessed
531 2012-09-15).
- 532 (35) Schindelin, J.; Arganda-Carreras, I.; Frise, E.; Kaynig, V.; Longair, M.; Pietzsch, T.;
533 Preibisch, S.; Rueden, C.; Saalfeld, S.; Schmid, B.; Tinevez, J.-Y.; White, D. J.;
534 Hartenstein, V.; Eliceiri, K.; Tomancak, P.; Cardona, A. Fiji: An Open-Source Platform for
535 Biological-Image Analysis. *Nature Methods* **2012**, *9* (7), 676–682.
536 <https://doi.org/10.1038/nmeth.2019>.
- 537 (36) Kessler, R. W.; Becker, U.; Kohler, R.; Goth, B. Steam Explosion of Flax - a Superior
538 Technique for Upgrading Fibre Value. *Biomass and Bioenergy* **1998**, *14* (3), 237–249.
- 539 (37) Minopoulou, E.; Dessipri, E.; Chryssikos, G. D.; Gionis, V.; Paipetis, A.; Panayiotou, C.
540 Use of NIR for Structural Characterization of Urea–Formaldehyde Resins. *International*
541 *Journal of Adhesion and Adhesives* **2003**, *23* (6), 473–484. [https://doi.org/10.1016/S0143-7496\(03\)00089-7](https://doi.org/10.1016/S0143-7496(03)00089-7).
- 542 (38) Benthien, J. T.; Heldner, S.; Ohlmeyer, M. Investigation of the Interrelations between
543 Defibration Conditions, Fiber Size and Medium-Density Fiberboard (MDF) Properties. *Eur.*
544 *J. Wood Prod.* **2017**, *75* (2), 215–232. <https://doi.org/10.1007/s00107-016-1094-2>.
- 545 (39) Bond, J.; Donaldson, L.; Hill, S.; Hitchcock, K. Safranin Fluorescent Staining of Wood
546 Cell Walls. *Biotechnic & Histochemistry* **2008**, *83* (3–4), 161–171.
547 <https://doi.org/10.1080/10520290802373354>.
- 548 (40) Grigsby, W. J.; Thumm, A.; Kamke, F. A. Determination of Resin Distribution and
549 Coverage in MDF by Fiber Staining. *WOOD AND FIBER SCIENCE* **2003**, *37*, 12.
- 550 (41) Loxton, C.; Thumm, A.; Grigsby, W. J.; Adams, T. A.; Ede, R. M. Resin Distribution in
551 Medium Density Fiberboard. Quantification of UF Resin Distribution on Blowline-and
552 Dry-Blended MDF Fiber and Panels. *Wood and Fiber Science* **2003**, *35*, 11.
- 553 (42) Thumm, A.; McDonald, A. G.; Donaldson, L. A. Visualisation of UF Resin in MDF by
554 Cathodoluminescence/ Scanning Electron Microscopy. *Holz als Roh- und Werkstoff* **2001**,
555 *59* (3), 215–216. <https://doi.org/10.1007/s001070100196>.
- 556 (43) Xing, C.; Riedl, B.; Cloutier, A.; Shaler, S. M. Characterization of Urea–Formaldehyde
557 Resin Penetration into Medium Density Fiberboard Fibers. *Wood Sci Technol* **2005**, *39* (5),
558 374–384. <https://doi.org/10.1007/s00226-005-0294-4>.
- 559
560

561 SYNOPSIS

562 This work presents an ecological solution for the recovery of MDF waste, a non-recyclable and
563 environmentally harmful material.

564

565